# SEISMIC RISK ASSESSMENT OF INTERDEPENDENT ELECTRIC POWER AND WATER SUPPLY SYSTEMS IN CHRISTCHURCH, NEW ZEALAND

I. Kongar[(1)], S. Giovinazzi[(2)], T. Rossetto[(3)]

[(1)] *Research Engineer, University College London, ucfbiko@ucl.ac.uk*
[(2)] *Senior Research Fellow, University of Canterbury, sonia.giovinazzi@canterbury.ac.nz*
[(3)] *Professor, University College London, t.rossetto@ucl.ac.uk*

## *Abstract*

This paper applies a generalized framework for modelling interdependent infrastructure system performance to a case study of the electric power and water supply systems in Christchurch, New Zealand. Based on geospatial exposure data provided by infrastructure operators, the case study identifies the key assets in each system and selects appropriate fragility functions. These are applied along with existing hazard prediction methods to first measure the performance of each system independently and then interdependencies are accounted for by two methods: supply area and proximity. A new interdependency response metric is proposed to measure the magnitude of the interdependency effect of electric power on water supply with minimal computation. For a 10,000-year stochastic earthquake catalogue the electric power network exhibits high resilience with system performance issues arising in less than 3% of events. Exceedance probability curves show that the water supply system is less resilient, due to the effect of ground shaking and liquefaction on pipelines, and that for this case study, the method for modelling interdependency makes little difference to the results. The interdependency metric calculated for each event is low in most cases. However, regression analysis shows a strong linear trend between the interdependency metric and the loss metric for the electric power network and this observation may be exploited in future to develop a simple method for predicting the interdependency effect between any two systems without full simulation.

*Keywords: Lifelines; Interdependencies; Seismic risk assessment; Critical infrastructure*

## 1. Introduction

Critical Infrastructure systems, which are also commonly known as lifelines, can be defined as the systems which provide for the circulation of peoples, good, services and information upon which health, safety, comfort and economic activity depend [1]. Lifelines systems include utility networks such as energy, water and telecommunications; transport systems such as roads; or discrete critical facilities such as hospitals, ports and airports. When an earthquake occurs, damage to lifelines can be caused directly by the hazard (e.g. ground shaking causing structural failure of a component), or indirectly due to interdependencies with other disrupted systems with which it is connected (e.g. loss of electric power could disrupt water supply infrastructure if no back-up supply is available to power pumping facilities). Furthermore, damage to lifelines has two main impacts: costs associated with repair of physical damage and disruption to people and businesses due to service interruption. This means that the resilience of lifelines depends on both structural performance and their capacity to provide their services [2]. Despite the important role lifeline damage and service interruption has on earthquake losses, analysis of the seismic performance of lifelines is given limited consideration by the insurance sector. This is partly due to the paucity of comprehensive data on earthquake-induced damage and loss of functionality of lifelines, which has made it difficult to create empirical damage models or calibrate analytical models. The research presented in this paper is part of a wider study aimed at improving how the seismic performance of lifelines is considered by the insurance industry with a focus on two engineering aspects: firstly the simulation of system performances for loss estimation; and secondly the quantification of interdependencies between systems as a strategic risk management metric.

The general procedure for seismic risk assessments of buildings has been established by earthquake engineers for over 40 years [3] and has been adopted by companies such as AIR Worldwide and Risk Management Solutions, RMS, who produce specialist catastrophe modelling software for the insurance industry [4]. The same basic procedure can be modified to apply to lifelines. The four basic components of seismic risk assessment include an exposure module, a hazard module, a vulnerability module and a loss module, as summarised by the flowchart in Fig.1, which is based on current lifelines earthquake engineering best practice in the SYNER-G study [5]. The exposure module classifies the lifelines and their constituent components so that elements that are expected to behave similarly are considered uniformly. It describes the physical characteristics of the assets at risk and information that will be used to measure losses e.g. asset replacement cost. The hazard module simulates the earthquake events. It is necessary to determine the appropriate earthquake hazard parameters against which damage should be evaluated and then generate local seismic hazard intensities at each site. The vulnerability module estimates the level of damage experienced by each asset, by first defining the appropriate scales for classifying damage and then identifying an appropriate hazard-damage relationship with which to assign damage to each asset based on the hazard intensity, similar to a fragility function. The loss module translates the damage into an estimate of the loss metric. From an engineering perspective, for lifelines the loss metric assesses the performance of the whole system based on the damages that have been assigned to each component within it. This can be static, at the time of the event, or it can consider how the performance changes with time after the earthquake if asset restoration times are modelled. These seven steps model the consequences of a single earthquake; however measures of risk should be probabilistic. Therefore steps 4 to 7 can be repeated for multiple scenario earthquakes and the distribution of loss metrics can be plotted in order to obtain a probabilistic view of risk to the systems. In applying these steps, there are some considerations that are specific to lifelines. In the hazard module, probabilistic seismic hazard assessment (PSHA) [6] is not appropriate for lifelines since they are spatially distributed and system performance can only be evaluated if seismic hazard is represented in terms of random fields accounting for the statistical dependencies between ground motion parameters [7, 8]. Also in the vulnerability module consideration must be given to both the physical and operational state of an asset, since the latter is necessary to model system performance.

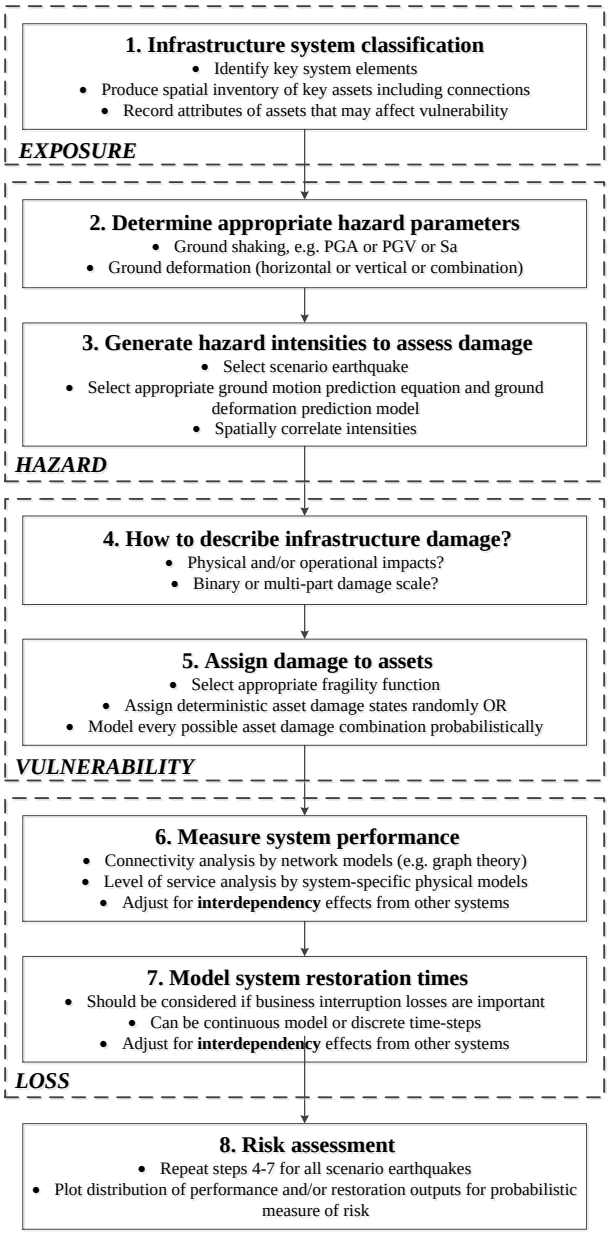


Fig. 1 – Flow chart for steps in seismic risk assessment of lifelines systems

The flow chart in Fig. 1 is a simple framework for the seismic risk assessment of lifelines for the insurance sector and is not intended to be a prescriptive methodology. There are alternative ways of interpreting the framework, which reflects that fact that different analysts may have different requirements in terms of accuracy and detail; varying resources might be allocated to the task; and different levels of access might be available to model input data. An application of the framework is demonstrated in this paper with a case study of the electric power and water supply systems in Christchurch, New Zealand. These two systems exhibit interdependency since the water supply system relies on electric pumps to extract water from underground aquifers and to pump water into elevated parts of the city. The objectives of the case study are to probabilistically estimate the seismic risk to the two systems in terms of a performance-related loss metric, and use the risk assessment as a means of quantifying the interdependency between the two systems. For the purposes of this research, a new interdependency response metric is proposed to quantify the dependence of one system on another as observed from a single event. For two systems, A and B, where B is dependent on A, the metric measures the reduction in post-earthquake performance of system B due solely to the loss of performance

in system A. This definition is based on the Leontief input-output method for modelling lifelines interdependencies [9] but accounts for the proportional rather than absolute reduction in performance of system B, which is advantageous when using loss metrics with an upper bound [10]. For the electric power and water supply systems in the case study, the formula for the metric, $I_{WS,EP}$, is given by Eq. 1, where $LM_{WS}$ is the loss metric calculated for the water supply system independently and $LM_{WS|EP}$ is the loss metric calculated for the water supply system when accounting for interdependencies. The loss metrics are defined in the following section.

$$I_{WS,EP} = \frac{LM_{WS|EP} - LM_{WS}}{100 - LM_{WS}} \tag{1}$$

## 2. Case study

### 2.1 Context

Christchurch is located in the Canterbury region on the South Island of New Zealand and is the second largest city in the country, with a population of around 350,000. The Canterbury earthquake sequence occurred between 2010 and 2011 and generated in excess of 10,000 individual seismic events, mostly of moderate magnitude. Although the purpose of this case study is to assess future risk, data and observations from the sequence, provided by Orion NZ Ltd and the University of Canterbury, are used for empirical model development [10, 11, 12], in particular the two most damaging events within the sequence: the initial $M_W$ 7.1 main shock on 4th September 2010 (the Darfield earthquake) and the $M_W$ 6.2 aftershock on 22nd February 2011 (the Christchurch earthquake). A context map of New Zealand and the locations of the epicentres of the two earthquakes in relation to the city of Christchurch are shown in Fig. 2.

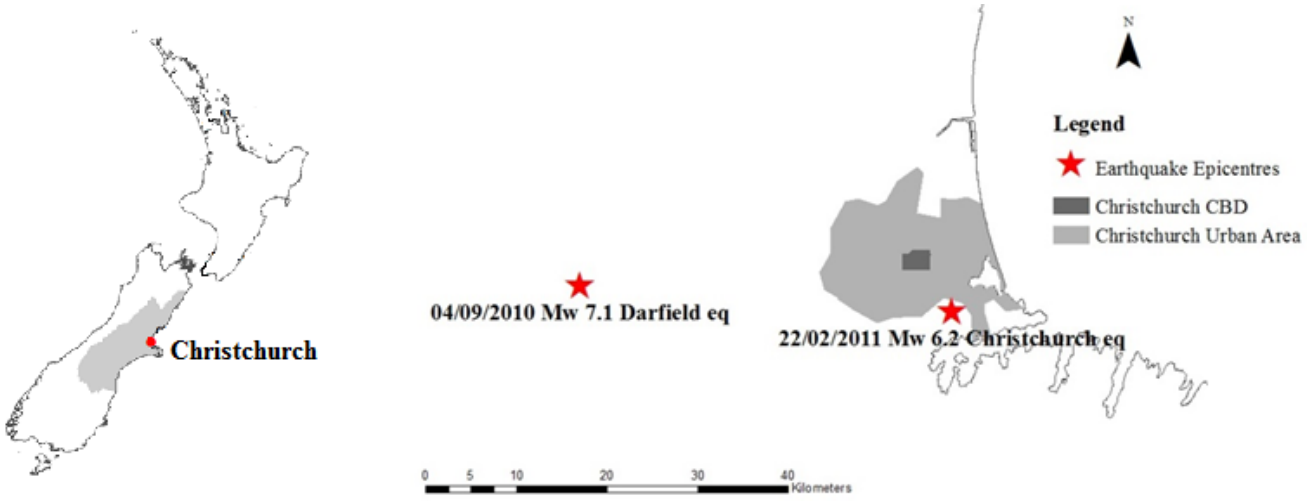


Fig. 2 – Map showing location of Christchurch within New Zealand (left) and epicentres of major events in Canterbury earthquake sequence relative to the urban area and Central Business District (CBD) (right)

### 2.2 Exposure

For the assessment of lifelines systems, the insurance industry is often limited in terms of the inventory data that can be accessed. Often only data that are available in the public domain can be studied, which means that only a simplified version of the network can be analysed. For the sub-transmission part of the

electric power network is considered. This includes five grid exit points (GXPs) on the edge of the city that receive power from the National Grid, 30 district/zone substations within the city itself and the overhead lines (97km) and buried cables (145km) that link the GXPs to the district/zone substations. The GXPs are substations that receive power at 220kV and transform this to 66kV, 33kV or 11kV before re-distributing into the sub-transmission network. The district/zone substations transform power to 11kV (if required) and re-distribute into the local distribution network. For buried cables, the main attribute affecting vulnerability is insulation material [11]. The predominant insulation types in Christchurch are: oil-filled cables; paper-insulated lead-covered armoured cables (PILCA); PILCA cables reinforced with high density polyethylene (PILCA HDPE); cross-linked polyethylene cables (XLPE); and polyvinyl chloride cables (PVC).

Drinking water is obtained by pumping through wells from underground gravel aquifers, which extend under the city and westwards under the Canterbury Plains, to depths of up to 220m. There are 56 extraction sites in the Christchurch urban area, housing a total 105 primary pumping stations, of which 43 had access to back-up power supply in the form of a diesel generator. Some pumping stations are linked to more than one well and there are a total of 147 wells. The system is supported by 32 booster pumps to provide water to the Port Hills area to the south of the city. None of the booster pumping stations have access to back-up power. Since the water supply network is very large (> 120,000 pipes), a simplified version of the network is considered in the case study including all pipes of diameter > 300mm and some smaller pipes as necessary to ensure that all pipes and booster pumps are connected to at least one well and that there are no isolated assets. The final network includes 270km of pipes constructed from a range of materials, although the most common are asbestos cement (AC, 109km), cement lined steel (CLS, 36km) and polyvinyl chloride (PVC, 31km).

## 2.3 Seismic Hazard

Seismic hazard is calculated probabilistically by means of a Monte Carlo simulation, with an artificial 10,000-year catalogue of earthquakes generated stochastically based on the New Zealand Seismic Hazard Model [13] and accounts for active faults and distributed seismicity within a 200km radius of Christchurch. There are 80 active faults in this region with defined location, characteristic magnitude and other physical attributes necessary for estimating intensities. For distributed seismicity the region is divided into seven source zones with a maximum magnitude and fault type. Earthquake records from GeoNet [14] are used to determine a Gutenberg-Richter *b*-value for each zone. Each zone is further sub-divided into a 10km x 10km grid and using the same records, a Gutenberg- Richter *a*-value is determined for each grid cell. The stochastic catalogue considers only earthquakes with $M_W \geq 5$ and so with the assumption that each distributed seismicity grid cell is effectively a unique source, there are 61,204 possible magnitude/source combinations with a composite occurrence rate of 1.45 earthquakes per year. The time between events in the stochastic catalogue is modelled with an exponential distribution under the assumption that the temporal occurrence of earthquakes is described by a Poisson process. By sampling a random number, $U$, from a uniform distribution between 0 and 1, the time to the next earthquake, $T$, in years can be generated by $T = \ln(U)/\lambda$, where $\lambda$ is the rate parameter, which is 1.45 events per year. The magnitude and source of the event are determined by weighted random sampling from all magnitude/source combinations, with weights equal to the annual rate of each combination. The study area is divided into a 1km x 1km grid of 294 cells for the calculation of intensities. The two hazards affecting lifelines are ground shaking and seismic-induced liquefaction. For ground shaking both peak ground acceleration (PGA) and peak ground velocity (PGV) are calculated, with the latter being most relevant for buried infrastructure such as pipes and cables since it relates to ground strain [15]. Liquefaction is measured in terms of horizontal permanent ground deformation ($PGDf_H$), representing lateral spread, and vertical permanent ground deformation ($PGDf_V$), representing differential vertical settlement.

PGAs are calculated using the ground motion prediction equation (GMPE) and accompanying standard deviation model of Bradley [16], which is a New Zealand-specific adaptation of the PEER-NGA model proposed by Chiou et al. [17]. PGVs are calculated from the original Chiou et al. model. For active faults, the geometric properties required to apply the GMPE are specified by the NZSHM. However, for distributed seismicity sources, only location and fault type are known, so the geometric properties are estimated based on guidelines proposed for dealing with unknown input parameters for PEER-NGA models [18]. A new Christchurch-specific

spatial correlation model for PGA intra-event residuals has been developed using GeoNet strong motion recordings [14] from four events in the Canterbury earthquake sequence: the Darfield earthquake; the Christchurch earthquake; the $M_W$ 5.9 earthquake on 13th June 2011; and the $M_W$ 5.8 earthquake on 23rd December 2011. The recordings provide 1,884 correlation observations, grouped into bins according to site separation distance. Six different functional forms are fit to the observed data and the exponential form [7] is found to minimize the least squares error for short separation distances (< 15km) at which spatial correlations are most important [10]. Spatially correlated fields of intra-event residuals are simulated using the matrix decomposition method proposed in the SYNER-G study [5]. To ensure that the final PGAs and PGVs are correlated, the sequential conditional simulation method proposed by SYNER-G [5] is applied.

The calculation of permanent ground deformations (PGDf) is a three-step process. First, the liquefaction susceptibility of a site is determined from the Christchurch liquefaction risk map [19]. If the site is deemed to be liquefiable, liquefaction triggering that accounts for PGA and soil properties is estimated. Kongar et al. [12] evaluated a range of simplified methods against observations from the Canterbury earthquake sequence and showed that the most accurate model for predicting liquefaction occurrence in Christchurch is the method proposed by Andrus and Stokoe [20] for calculating liquefaction potential index (LPI) from shear wave velocity profiles. This method is applied in the case study with an LPI value of 4 used as a threshold for liquefaction occurrence. If liquefaction is predicted to occur at a site, horizontal lateral spread deformation ($PGDf_H$) and vertical settlement deformation ($PGDf_V$) are calculated using the Hazus methods [21].

## 2.4 Vulnerability

Since this seismic risk assessment focuses on connectivity, the objective of the vulnerability analysis is to determine the probability that an asset will suffer functional failure. For the purposes of comparison with existing fragility functions, it is assumed that operational failure is equivalent to the 'Extensive' damage state defined by Hazus [21]. The two vulnerable elements in the electric power network are substations and conduits. The existing Hazus fragility function for 'Extensive' damage for low voltage substations is inadequate for assessing the vulnerability of substations in Christchurch as they significantly over-predict functional failures compared to observations from the Canterbury earthquake sequence [10]. Since there are insufficient data from these earthquakes to develop completely new empirical fragility functions (in terms of number of damage observations and PGA range), the observations are used to update the existing Hazus fragility function using Bayesian techniques as proposed by the Global Earthquake Model [22]. For ground shaking hazard, a function is produced in terms of PGA and for liquefaction hazard separate functions are produced in terms of $PGDf_H$ and $PGDf_V$. For conduits it is generally considered that the operability of overhead lines is not vulnerable to earthquakes [23] and this view is supported by evidence from the Canterbury earthquake sequence [24]. Buried cables are however vulnerable, especially to liquefaction [24] and so empirical repair rate functions have been developed for buried cables based on damage observations from the Darfield and Christchurch earthquakes [11]. The repair rate functions predict the mean number of repairs per unit length based on $PGDf_{GEOM}$ (the geometric mean of $PGDf_H$ and $PGDf_V$) and different functions are produced for different insulation materials. The new functions for substations and buried cables are shown in Table 1.

In the water supply network the three vulnerable elements are pipes, wells and booster pumps. For pipes new repair rate functions have been produced based on damage observations from the Christchurch earthquake and different functions produced for different pipe materials with PGV and PGDf as intensity measures [10]. For wells and booster pumps, existing Hazus fragility functions for 'Extensive' damage over-predict functional failures when compared to observations from the Canterbury earthquake sequence but the observations are insufficient in terms of number and PGA range to create new functions. Therefore observations from the Darfield and Christchurch earthquakes are used to update the Hazus functions using Bayesian procedures [10]. For $PGDf_H$ and $PGDf_V$, the same functions are proposed as for substations. This reflects the fact that Hazus uses the same liquefaction hazard fragility functions for all infrastructure nodes. The new functions for wells, pumping stations and pipelines are shown in Table 1.

Table 1 – Fragility (functional failure) and repair rate functions derived for Christchurch case study

| Asset | Function | Notes |
|---|---|---|
| Buried cables [11] | $RR = K_1 \times \left(4.317 PGDf_{GEOM} - 0.325\right)$ | For PILCA, $K_1 = 1$, for PILCA HDPE, $K_1 = 0.82$, for XLPE, $K_1 = 0.26$, for other types, $K_1 = 1.07$ |
| Pipes [10] | $\log RR = K_2 \log PGV - K_3$ | For AC, $K_2 = 2.489$, $K_3 = 4.359$, for brittle, $K_2 = 2.77$, $K_3 = 4.826$, for ductile, $K_2 = 2.853$, $K_3 = 5.173$ |
| Pipes [10] | $\log RR = 0.639 \log PGDf_{GEOM} + 0.976$ | For AC pipes only |
| Pipes [10] | $RR = K_4 PGDf_{GEOM} + K_5$ | For brittle, $K_4 = 8.294$, $K_5 = 2.312$, for ductile, $K_4 = 2.937$, $K_5 = 0.564$ |
| Nodes [10] | $P\left[ fail \mid PGA \right] = \Phi\left[ \frac{1}{\beta} \ln\left( \frac{PGA}{\mu} \right) \right]$ | For substations, $\mu = 1.132$, $\beta = 0.428$, for wells, $\mu = 1.385$, $\beta = 0.876$, for booster pumps, $\mu = 1.216$, $\beta = 0.604$ |
| Nodes [10] | $P\left[ fail \mid PGDf_H \right] = \Phi\left[ \frac{1}{1.539} \ln\left( \frac{PGDf_H}{1.029} \right) \right]$ | Same for all nodes |
| Nodes [10] | $P\left[ fail \mid PGDf_V \right] = \Phi\left[ \frac{1}{1.176} \ln\left( \frac{PGDf_V}{0.477} \right) \right]$ | Same for all nodes |

In each earthquake simulation, every asset is assigned to a single functional state and assessed as being either functional or non-functional. For infrastructure nodes, the failure probability of the asset for each individual hazard is calculated from the fragility functions according to the corresponding intensities and then the overall failure probability accounting for all hazard types is given by Eq. 2, which is the method adopted by Hazus [21] and assumes that the failure probabilities due to ground shaking and liquefaction are independent.

$$P\left[ fail \right] = 1 - \left(1 - P\left[ fail \mid PGA \right]\right) \times \left(1 - \max\left\{ P\left[ fail \mid PGDf_V \right]; P\left[ fail \mid PGDf_H \right] \right\}\right) \quad (2)$$

The functionality of the asset is then assigned by randomly sampling from a uniform distribution between 0 and 1, and comparing the sampled variate to the asset failure probability. The asset is assumed to have failed and therefore be non-functional if the variate is less than or equal to the failure probability, and is assumed to be functional otherwise. In the case of linear assets, the mean repair rate for a section of cable or pipe is calculated from the relevant function. Assuming that the distance between repairs along a section of cable/pipe can be modelled as a Poisson distribution [25] with rate parameter equal to the calculated repair rate, then the probability of at least one repair occurring on the section is evaluated. For cables this is equivalent to the probability of failure and functionality can then be assigned in the same way as for the nodes. For pipes this is equivalent to the probability of damage, which can either be a break or a leak. Only a break causes loss of connection and so the Hazus assumption is adopted that in areas of liquefaction, the probability of a repair being a break is 0.8 and in areas where there is no liquefaction, the probability of a repair being a break is 0.2. The probability of at least one repair on a pipe is multiplied by the relevant break probability to determine the failure probability and functionality can then be assigned in the same way as for the nodes.

## 2.4 Loss and Interdependency Quantification

The loss metric adopted for both systems in this case study is the percentage of customers disconnected from the network after each event. For the electric power network, each district/zone substations act has a defined supply area and so each substation acts as a demand node. The population served within each supply area is determined from night time population data from the 2013 Census [26]. The total population in the study area is 328,814. Meshblocks are the smallest geographic unit for which statistical data is collected in New Zealand and there are 3,352 in the study area. It is assumed that a meshblock is supplied by a particular substation if the meshblock's

centroid falls within the substation's supply area. In some locations the supply areas overlap, meaning that some meshblocks can be supplied by more than one substation. After an earthquake, it is assumed that the entire population of a meshblock is connected to the power network if at least one of its supply substations remains operational, i.e. the substation is undamaged physically and there is an undamaged path between the substation and at least one operational GXP.

For the water supply system, a manual approach is required to create demand nodes since there is no single feature like the district/zone substations that cover the full study area extents. Each booster pump is treated as a demand node and demand nodes are also created at all network endpoints (i.e. where a 300mm diameter pipe connects to a smaller pipe). To increase the resolution of the analysis, some additional demand nodes are created at intermediate pipe junctions. These additional nodes are located subjectively based on factors including population density and meshblock size so that there are more sinks in more densely developed areas. In total 340 demand nodes are created. Each meshblock is assigned to a single demand node. Visual inspection of the pipe layout downstream of each booster pumps allows the supply area of each pump to be easily identified. A meshblock is assigned to either a booster pump demand node, if it falls within the supply area of a booster pump, or otherwise it is assigned to the closest non-pump demand node. Each meshblock is only assigned to a single demand node. The entire population of a meshblock is deemed to be connected to the water network if there is an undamaged path between its assigned demand node and any operational well. Where a meshblock is assigned to a booster pump sink node, the booster pump must also itself be operational.

To demonstrate the importance of lifelines interdependency a comparison is made between loss metrics calculated with and without accounting for interdependencies. The loss metrics are calculated initially for each system independently and then subsequently repeated for the water supply system to account for its dependence on electric power. In the independent analysis, a pump is assumed to be non-operational only if it is directly physically damaged. In the interdependent analysis, a pump can be non-operational if it is either physically damaged or if it loses its networked power supply and does not have access to a back-up generator. To account for this phenomenon, each pump is assigned to one or more district/zone substation. The case study tests two different methods for assigning pumps to supply areas. The first and simplest method, used in studies such as SYNER-G [5] is to assign each pump to the closest substation. This means each pump is only assigned to a single substation with no power supply redundancy. The second method is to assign a pump to all substations whose supply area it falls inside, which better reflects the real situation in terms of redundancy and actual system inter-connection. Finally a value for the interdependency response metric is calculated for each event in the 10,000-yr catalogue and the distribution of these values in analysed using statistical regression techniques to determine trends in the system interactions.

## 3. Results

The application of the seismic hazard model generates 14,428 events of $M_W \geq 5$ for the 10,000-yr catalogue, although in 2,278 years there are no events. The seismic risk assessment shows that the electric power network only suffers a loss of performance in 228 of the events. Whilst there are some additional events in which damage is observed amongst electric power assets, the provision of redundancy in the network means that this damage does not result in any customers being disconnected. The distribution of the loss metric for the 228 performance-affecting events is shown in Fig. 3. In the majority of these events, the disruption to customers is relatively low (<25%), although there are a small number of events that do cause major disruption to the system. The reliability demonstrated by the electric power network can be explained by two factors. Firstly, following observations of damage to substations caused by the 1987 Edgecumbe earthquake, substations in Christchurch have been seismically reinforced [27]. This means that very high accelerations are needed to cause sufficient damage to induce failure. Secondly, only buried cables are considered to be vulnerable to earthquake damage, and even then, they are only considered to be susceptible to damage caused by liquefaction, which in turn requires high accelerations. Damage to substations and buried cables are therefore only likely to occur due to high magnitude earthquakes or moderate magnitude earthquakes close to the city. The water supply system is less reliable than the electric power network, since every event causes some loss of performance even when interdependencies are not taken into account. The median values for the fragility functions for water supply system nodes indicate that

in general very high accelerations are needed to cause damage to these assets. The main cause of vulnerability in this system is therefore likely to be the pipelines, in particular because they are susceptible to ground shaking as well as to liquefaction and so are inherently more vulnerable than buried cables. This vulnerability was observed in the Canterbury earthquake sequence and is reflected in the repair rate functions derived for this study. On average, compared to independent system analysis, modelling interdependency by supply area increases the loss metric by 7.7%, whilst modelling interdependency by proximity increases the loss metric by 5.2%. Fig. 4 presents risk curves for each system, which plot the annual exceedance probabilities corresponding to different values of the loss metric. To calculate the probabilities, the distribution of loss metrics is annualised by taking the maximum occurrence in each year of the catalogue. In the insurance sector it is more common to identify the loss metrics corresponding to specified return periods [4]. The dots on each curve in Fig. 4 represent the following return periods, measured in years: 5, 10, 20, 50, 100, 200, 500, 1,000, 2,000, 5,000 and 10,000.

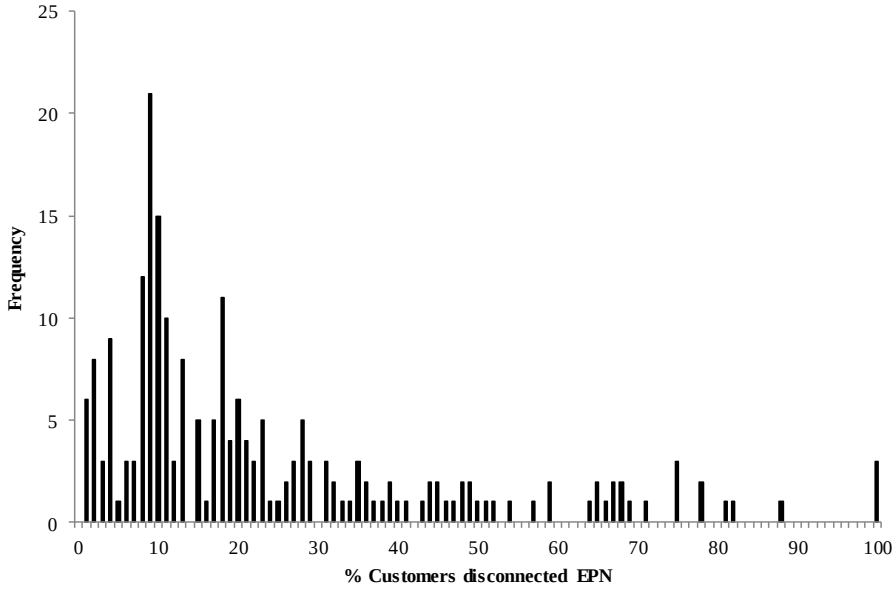


Fig. 3 – Distribution of loss metric for events that affect the performance of the electric power network

The EP curves confirm that for this case study the difference in loss metrics between the three interdependency modelling scenarios is small and almost negligible at low return periods (< 100 years). The curves also highlight that whilst the electric power network is generally very reliable, significant disruption is expected for high return period events. The interdependency response metric, *I*, has been calculated for the 228 events in which interdependency was a factor. In 166 of the events the metric is less than 0.1 and in a further 32 events it is less than 0.2. The index exceeds 0.5 in only two of the events, which indicates that in general the effect of electric power interdependency on the water supply system is low. Potential trends in the value of the interdependency response metric have been investigated by plotting the calculated indices against the loss metric for the electric power network and the loss metric for the water supply system without interdependency analysis. The plots are shown in Fig. 5. Both plots show a trend for the degree of interdependency increasing as the loss metric increases as expected, although visually there appears to be more scatter amongst the data points in the plot for the water supply loss metric, suggesting there is a greater correlation between the interdependency response metric and the electric power loss metric. Linear regression has been applied to both plots to derive predictive functions for the interdependency response metric based on the loss metrics and the R-squared values for the fitted models further indicate that the electric power model has a better fit. The electric power loss metric explains approximately 80% of the variance compared to just over 60% for the water supply loss metric. The intercept of the electric power function is very close to zero, which follows the network logic since the interdependency response should be zero if there is no loss of performance in the electric power network. A

consequence of this is that the gradient of the best fit line can therefore be interpreted as a measure of the expected interdependency response in the water supply system when there is total failure in the electric power network. This is an objective metric for quantifying the resilience of the water supply system to power outages as a single value that is independent of any specific event and is therefore useful for high-level risk management and emergency planning purposes.

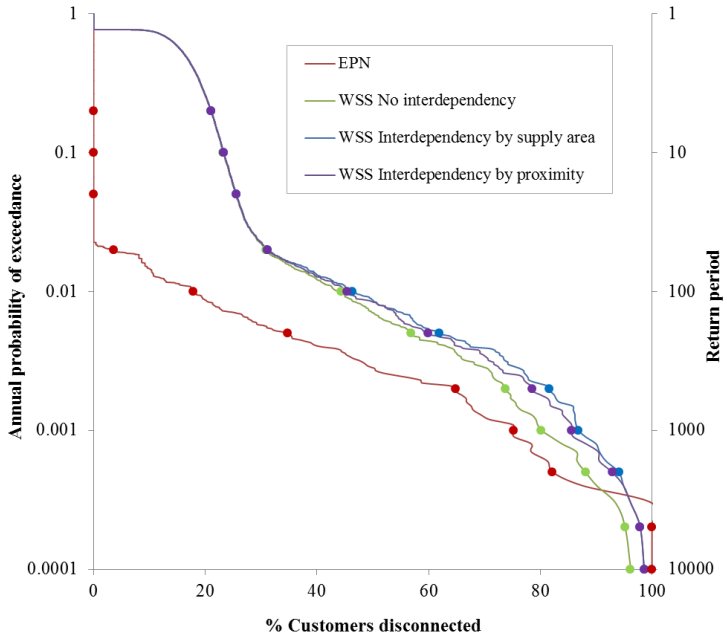


Fig. 4 – System risk curves for Christchurch electric power and water supply systems

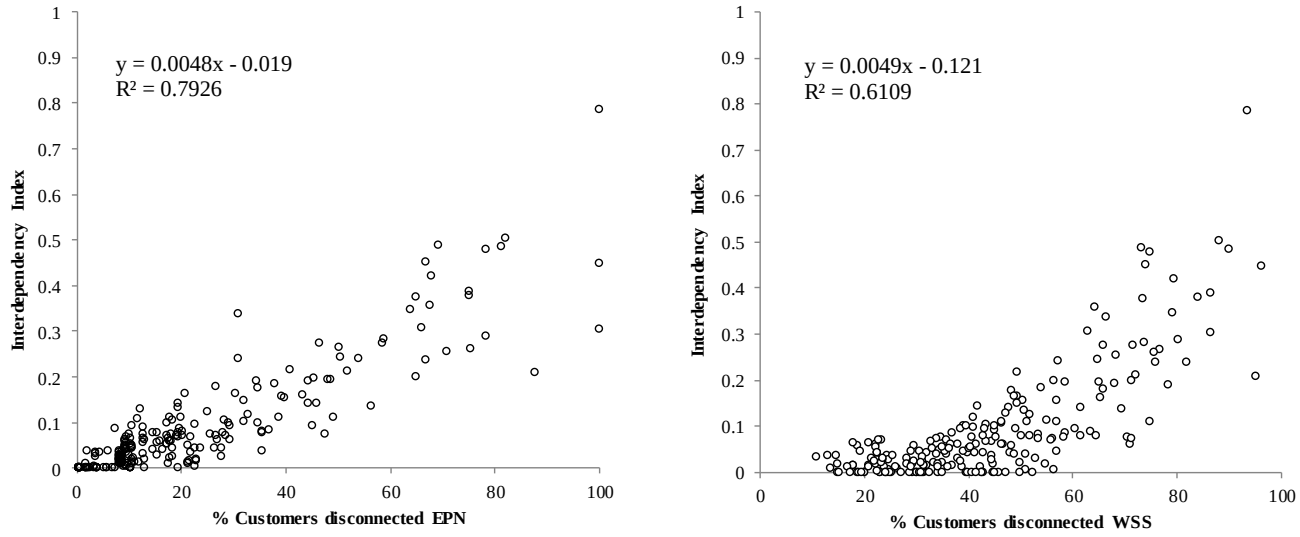


Fig. 5 – Plots of observed interdependency indices against electric power network (left) and water supply system (right) performance metrics

## 4. Conclusions

This research applies an existing seismic risk assessment framework for lifelines to a case study of the electric power and water supply systems in Christchurch, New Zealand. The application focuses on the problem of interdependencies and proposes a metric to evaluate the effect of interdependencies. The risk assessment has shown that for this specific study the electric power network is very reliable and able to maintain good performance levels after most events. The assets are primarily affected by earthquakes that cause high ground shaking and less than 3% of earthquakes in the catalogue cause performance issues. The water supply system is less reliable since pipelines are more susceptible to damage induced by ground shaking. Analysis of interdependencies has been constrained by the limited number of events in which the electric power network experienced loss of performance. Whilst the occurrence exceedance probability curves show that analysis of the water supply system without interdependencies underestimates risk at high return periods, there is little difference between the supply and proximity modelling methods, although this conclusion is currently specific to this case study and cannot be extended to other case studies without further research. An equation for measuring the degree of interdependency between two systems based on loss metrics has been proposed and has been applied to the events in the simulation, showing that in most events the effect of interdependency is evident but low. Regression analysis of the calculated values confirms that the performance of the electric power network is a good indicator for the degree of interdependency in an event and that a linear function provides a good fit. The gradient of the linear function also provides a more general event-independent measure of the relationship between the two systems. Two further pieces of analysis are required to build on this work. Firstly to determine whether this functional form is more generally applicable to any two interdependent systems, A and B, where B is dependent on A; and secondly, whether it is possible to develop a more efficient method for deriving the function that does not require a full seismic risk assessment. This case study has shown that whilst seismic risk assessment can be used to quantify interdependency, the analysis can be computationally intensive and yield only a small number of observations, particularly at high values for interdependency index and loss metric. It is at these high values that the effect of interdependency is most significant and so a more efficient method would be beneficial, particularly in cases where interdependency quantification is the primary objective and probabilistic risk assessment is not necessary.

## 5. Acknowledgments

The authors are grateful John O'Donnell, Shane Watson, Peter Elliott, Dave Brannigan and Ricki-Lee Teague at Orion New Zealand for the electric power network data and Matthew Hughes at the University of Canterbury for the water supply system data. Funding for this research project has been provided by the Engineering and Physical Sciences Research Council in the UK and the Willis Research Network and distributed through the Urban Sustainability and Resilience program at University College London.

## 6. References

[1] Platt, R (1991): Lifelines: an emergency management priority for the United States in the 1990s. *Disasters*, **15**(2), 172-176.

[2] Kongar, I, Esposito, S, Giovinazzi S (2015): Post-earthquake assessment and management for infrastructure systems: learning from the Canterbury (New Zealand) and L'Aquila (Italy) earthquakes. *Bulletin of Earthquake Engineering*, doi: 10.1007/s10518-015-9761-y

[3] Reitherman, R (1995): A review of earthquake damage estimation methods. *Earthquake Spectra*, **1**(4), 805-847.

[4] Grossi, P, Kunreuther, H (2005): *Catastrophe Modeling*. Springer.

[5] Pitilakis, K, Franchin, P, Khazai, B, Wenzel, H (2014): *SYNER-G: Systemic Seismic Vulnerability and Risk Assessment of Complex Urban Utility Lifeline Systems and Critical Facilities*. Springer.

[6] Cornell, CA (1968): Engineering seismic risk analysis. *Bulletin of the Seismological Society of America*, **58**(5), 1583-1606.

[7] Jayaram, N, Baker JW (2009): Correlation model for spatially distributed ground-motion intensities. *Earthquake Engineering & Structural Dynamics*, **38**, 1687-1708.

[8] Esposito, S, Iervolino, I (2011): PGA and PGV spatial correlation models based on European multievent datasets. *Bulletin of the Seismological Society of America*, **101**(5), 2532-2541.

[9] Haimes, YY, Jiang, P (2001): Leontief-based model of risk in complex interconnected infrastructures. *Journal of Infrastructure Systems*, **7**(1), 1-12.

[10] Kongar, I (2016): **S**eismic risk assessment of complex urban critical infrastructure networks. EngD Thesis, University College London.

[11] Kongar, I, Giovinazzi, S, Rossetto, T (2016): Seismic performance of buried electrical cables: evidence-based repair rates and fragility functions. *Bulletin of Earthquake Engineering*, Submitted.

[12] Kongar, I, Rossetto, T, Giovinazzi, S (2016): Evaluating simplified methods for liquefaction assessment for loss estimation. *Natural Hazards and Earth System Science*, doi: 10.5194/nhess-2016-281, Under review.

[13] Stirling, M, McVerry, G, Gerstenberger, M, Litchfield, N, van Dissen, R, Berryman, K, Barnes, P, Wallace, L, Villamor, P, Langridge, R, Lamarche, G, Nodder, S, Reyners, M, Bradley, B, Rhoades, D, Smith, W, Nicol, A, Pettinga, J, Clark, K, Jacobs, K (2012): National Seismic Hazard Model: 2010 update. *Bulletin of the Seismological Society of America*, **102**(4), 1514-1542.

[14] GeoNet, https://www.geonet.org.nz/, GNS Science

[15] Pineda-Parros, O, Najafi, M (2010): Seismic damage estimation for buried pipelines: challenges after three decades of progress. *Journal of Pipeline Systems Engineering*, **1**, 19-24.

[16] Bradley, B (2013): A New Zealand-specific pseudospectral acceleration ground-motion prediction equation for active shallow crustal earthquakes based on foreign models. *Bulletin of the Seismological Society of America*, **103**(3), 1801-1822.

[17] Chiou, B, Youngs, R, Abrahamson, N, Addo, K (2010): Ground motion attenuation model for small-to-moderate shallow crustal earthquakes in California and its implications on regionalization of ground-motion prediction models. *Earthquake Spectra*, **26**(4), 907-926.

[18] Kaklamanos, J, Baise, L, Boore, D (2011): Estimating unknown input parameters when implementing the NGA ground-motion prediction equations in practice. *Earthquake Spectra*, **27**(4), 1219-1235.

[19] Brackley, HL (2012): Review of liquefaction hazard information in eastern Canterbury, including Christchurch City and parts of Selwyn, Waimakariri and Hurunui districts. *Report No. R12/83*, Environment Canterbury.

[20] Andrus, RD, Stokoe, KH (2000): Liquefaction resistance of soils from shear-wave velocity. *Journal of Geotechnical and Geoenvironmental Engineering*, **126**(11), 1015-1025.

[21] Federal Emergency Management Agency: Mitigation Division (2015): *Hazus-MH2.1Earthquake Model technical Manual*. Department of Homeland Security, Washington DC, USA.

[22] Rossetto, T, Ioannou, I, Grant, D, Maqsood, N (2014): Guidelines for Empirical Vulnerability Assessment. *GEM Technical Report 2014-X*, GEM Foundation, Pavia, Italy.

[23] Vanzi, I (1996): Seismic reliability of electric power networks: methodology and application. *Structural Safety*, **18**(4), 311-327.

[24] Kwasinski, A, Eidinger, J, Tang, A, Tudo-Bornarel, C (2014): Performance of electric power systems in the 2010-11 Christchurch, New Zealand, earthquake sequence. *Earthquake Spectra*, **30**(1), 205-230.

[25] Adachi, T, Ellingwood, B (2008): Serviceability of earthquake-damaged water systems: effects of electrical power availability and power backup systems on system vulnerability. *Reliability Engineering & System Safety*, **93**(1), 78-88.

[26] Statistics New Zealand, *2013 Census*, http://www.stats.govt.nz/Census/2013-census.aspx

[27] Giovinazzi, S, Wilson, T, Davis, C, Bristow, D, Gallagher, M, Schofield, A, Villemure, M, Eidinger, J, Tang, A (2011): Lifelines performance and management following the 22 February 2011 Christchurch earthquake, New Zealand: highlights of resilience. *Bulletin of the New Zealand Society for Earthquake Engineering*, **44**(4), 402-417.